JOURNAL OF MATERIALS SCIENCE **39** (2004) 4481–4486

The stress transfer efficiency of a single-walled carbon nanotube in epoxy matrix

K. Q. XIAO, L. C. ZHANG
School of Aerospace, Mechanical and Mechatronic Engineering, The University of Sydney, NSW 2006, Australia
E-mail: zhang@mech.eng.usyd.edu.au

This paper investigates the effects of tube length and diameter on the distributions of tensile stress and interfacial shear stress of a single-walled carbon nanotube in epoxy matrix. It was shown that a smaller tube diameter has a more effective reinforcement and there exists an optimal tube length at which reinforcement is maximized. It was also found that a carbon nanotube has a greater stress transfer efficiency than a solid fibre, providing flexibility for toughness and tensile strength optimization. © *2004 Kluwer Academic Publishers*

1. Introduction

The low density of defects and high strength of the carbon-carbon sp^2 bonds give carbon nanotubes (CNT) the highest axial strength and modulus among all existing whiskers. Recent theoretical calculations and direct experimental measurements showed that the elastic modulus of a CNT is in the range of 1–5 TPa [1–3], which is significantly higher than that of a carbon fibre, from 0.1 to 0.8 TPa [4]. Such superior mechanical properties make CNTs a promising reinforcing material. If CNTs can have a large interfacial bonding strength with a matrix material, a great load transfer ability can be achieved, because a strong bonding allows shear stress to build up without causing interfacial failure. Some studies on a number of CNT-reinforced polymer composites have discussed the CNT-matrix interfacial bonding strength. For example, Wagner and coworkers [5–8] claimed that a strong CNT-polymer adhesion and a high interfacial bonding strength in a CNT/polyurethane system [6] could be possibly attributed to a "2 + 2" cycloaddition reaction between the tube and the polymer. By extending the traditional Kelly-Tyson model [9], Wagner [5] suggested that the interfacial bonding strength in a CNT composite might be higher than that in a fibre-reinforced composite, although this model is unable to demonstrate the distribution of the tensile and interfacial shear stresses along a tube under an external loading. Liao and Li [10] used molecular mechanics to simulate a pull-out process in a Single-Walled Nanotube (SWNT)/polystyrene system and reported that the interfacial bond strength could be up to 160 MPa even without considering the chemical bonding between the tube and matrix. Qian and coworkers [11, 12] found a significant load transfer ability of CNTs under tension. Recent work [13, 14] on the direct experimental measurement of bonding strength also showed remarkably high adhesion between a multi-walled nanotube (MWNT) or a SWNT and polymer. However, in a transmission electron microscopy study of an aligned nanotube/epoxy composite, Ajayan *et al.* [15] indicated that the interfacial bonding between a MWNT and epoxy matrix was weak. Schadler *et al.* [16], using Raman spectroscopy, also concluded that the interfacial bonding was very weak when a MWNT/epoxy composite was under tension. Some investigations also showed that interfacial bonding strength increased either with increasing the nanotube wall thickness [17] or with the formation of cross-links [18].

Previous investigations have mainly focused on the interfacial bonding strength. However, the dimensions of a nanotube can also influence its load transfer ability. To obtain a deeper understanding, the present study will use a modified Cox model to investigate the effects of length and diameter of a single-walled nanotube (SWNT) in an epoxy matrix on the load transfer properties.

2. Stress transfer

2.1. Modeling

The Cox model [19, 20] for a solid fibre, assuming a perfect interfacial bonding, can be extended to a hollow SWNT shown in Fig. 1. This gives rise to the following formulae for calculating the tube's tensile stress, σ_t, and interfacial shear stress, τ, along the longitudinal axis of the SWNT:

$$\sigma_t = E_t e\left[1 - \frac{\cosh\beta(L/2 - x)}{\cosh\beta L/2}\right] \tag{1}$$

$$\tau = \frac{E_t e A_t \beta}{2\pi r_2} \times \frac{\sinh\beta(L/2 - x)}{\cosh\beta L/2} \tag{2}$$

$$\beta = \sqrt{\left(\frac{G_m}{E_t}\right)\left(\frac{2\pi}{A_t \ln(R/r_2)}\right)} \tag{3}$$

where e is the strain externally applied on the SWNT composite in the axial direction of the tube, L is the length of the nanotube, G_m is the shear modulus of the matrix, E_t is the Young's modulus of the tube, R is a constant determined by the volume fraction of the nanotubes in the composite, $A_t = \pi(r_2^2 - r_1^2)$ is the area of the tube cross-section, and r_1 and r_2 are the inner and outer radii of the tube, respectively. The above formulae will reduce to the original Cox model when r_1 approaches zero.

In the following calculations, we take $E_t = 1.2$ TPa, $G_m = 1.2$ GPa, $e = 1\%$ and $R/r_2 = 600$ (a typical value used in fibre-reinforced composites), where $R/r_2 = (\pi/4V_f)^{1/2}$ is a parameter related to the nanotube volume fraction V_f. The effective wall thickness of a SWNT, $t = r_2 - r_1$, is a questionable quantity because a nanotube does not have a continuous wall. In the literature, t was often taken as 0.34 nm [21], the spacing between two adjacent graphite sheets. The authors believe that this cannot be true because the effective

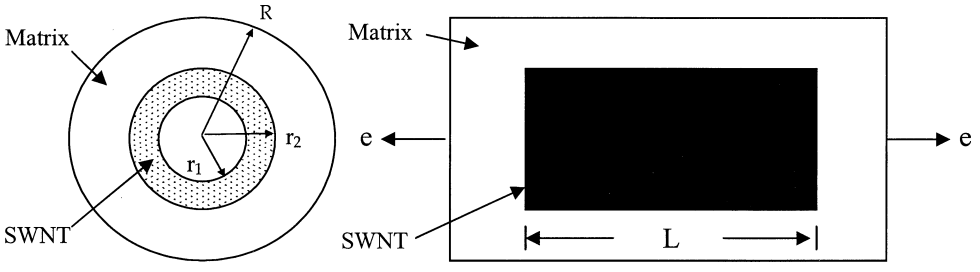

Figure 1 Schematic representation of a single SWNT composite cylinder under applied strain e. It is assumed that no epoxy is filled inside the nanotube.

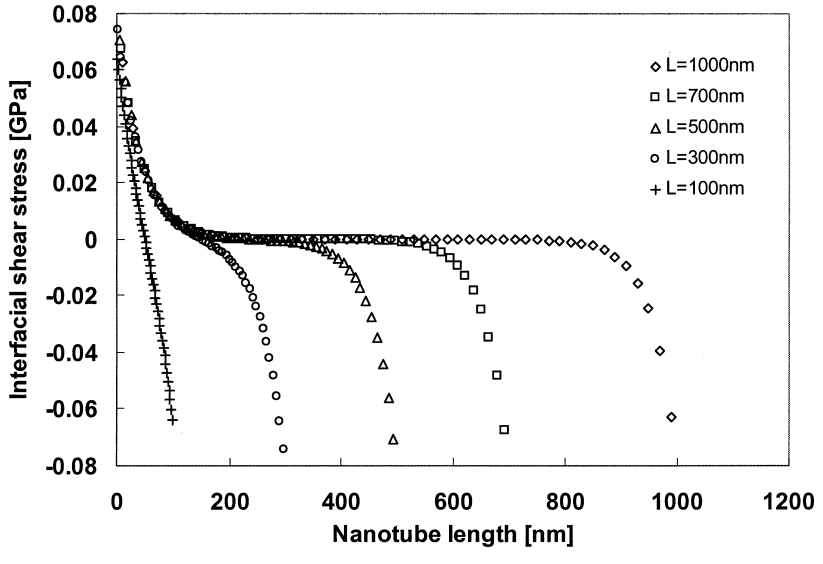

Figure 2 Shear stress at the SWNT/epoxy interface along the tube length ($d = 2$ nm and $t = 0.34$ nm).

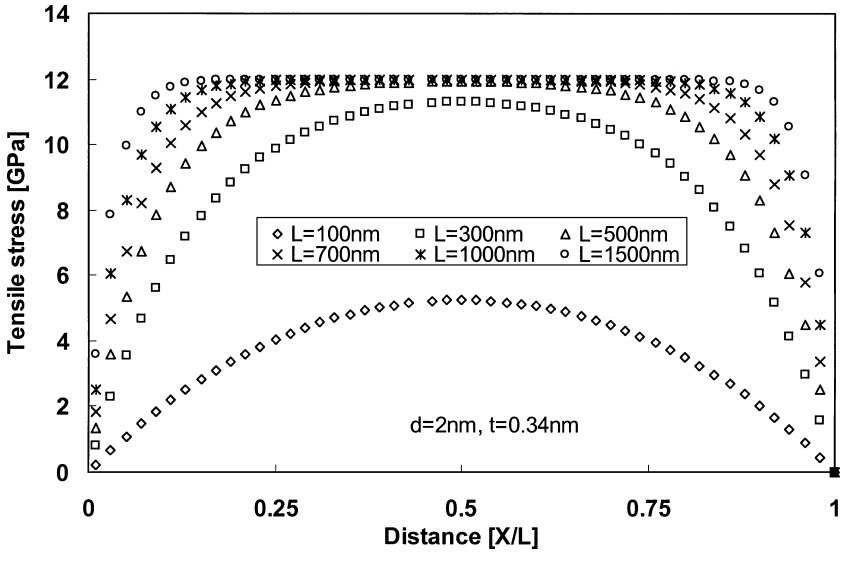

Figure 3 Tensile stress distributions at various tube lengths.

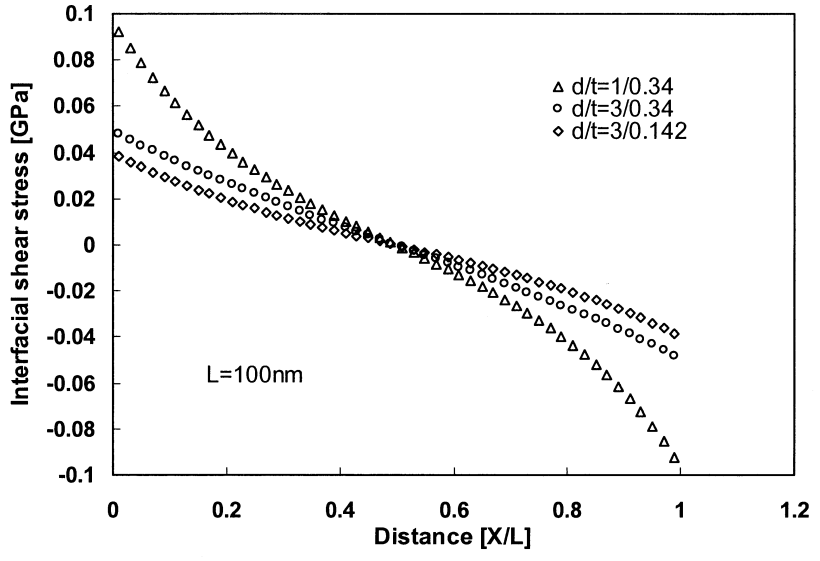

(a) L=100nm

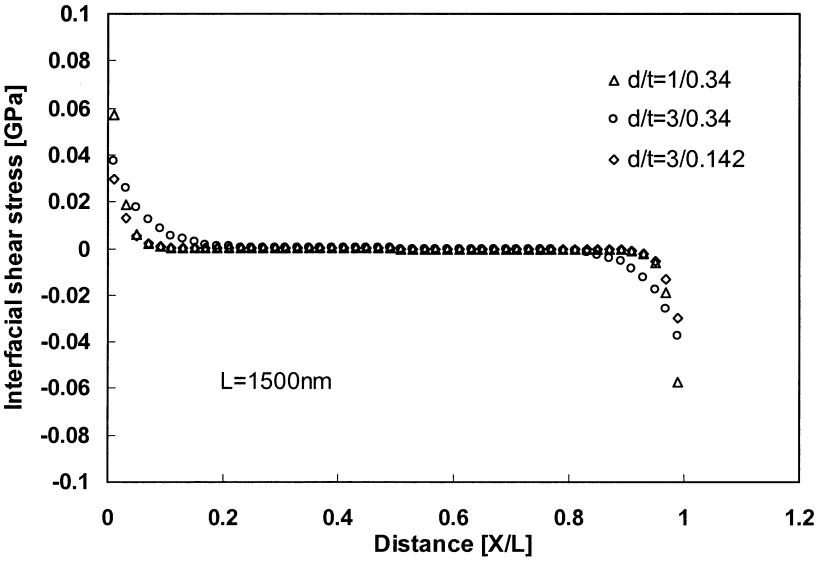

(b) L=1500nm

Figure 4 Effects of tube diameter d and wall thickness t on the interfacial shear stress (a) $L = 100$ nm and (b) $L = 1500$ nm.

wall thickness is a continuum mechanics quantity and hence its maximum value should be smaller than the theoretical diameter of a carbon atom if the equilibrium of a tube cross-section is considered [22]. For convenience, in this work, two wall thickness values, $t = 0.34$ nm and $t = 0.142$ nm (carbon atom covalent diameter [23]) are used to examine the thickness effect.

2.2. Stress distribution

The distribution of the shear stress along a tube of diameter $d = 2r_2 = 2$ nm is shown in Fig. 2. The shear stress has its maximum value, τ_{tmax}, at the two tube ends and is zero at the middle. Fig. 3 shows that the tensile stress starts to build up at the two ends of the nanotube and reaches its maximum, σ_{tmax}, at the middle. Increasing L increases σ_{tmax} when $L = 500$ nm σ_{tmax} becomes uniform and reaches nearly $E_t e$. Thus to have an effective reinforcement, L must be sufficiently long to make full use of the high tensile strength of a CNT. The above variations of the shear and tensile stresses along the nanotube axis indicate that the interfacial bonding failure between a CNT and its surrounding matrix must start from the tube's two ends. If the bonding strength is good enough, then the breaking of the nanotube should be at the middle of the tube.

Figs 4 and 5 show the effects of diameter and wall thickness of a nanotube on the distributions of the stresses. It is seen that an increase in d leads to a decrease in τ_{tmax} and τ_{tmax}. On the other hand, increasing t increases interfacial shear stress and decreases tensile stress. The effects of d and t become more obvious when the tube length is small.

2.3. Reinforcement

Suppose that a composite consists of a set of many parallel single composite cylinders with mean centre to centre separation of $2R$, the total number of nanotubes, m, in the composite is determined by

$$m = \frac{V_c}{4R^2L} = \frac{V_c}{4 \times 600^2 \times r_2^2 L} \tag{4}$$

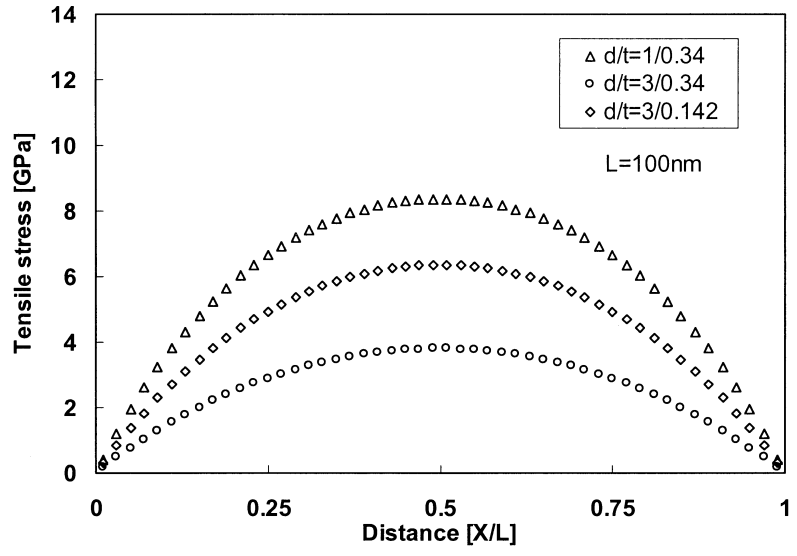

(a) L=100nm

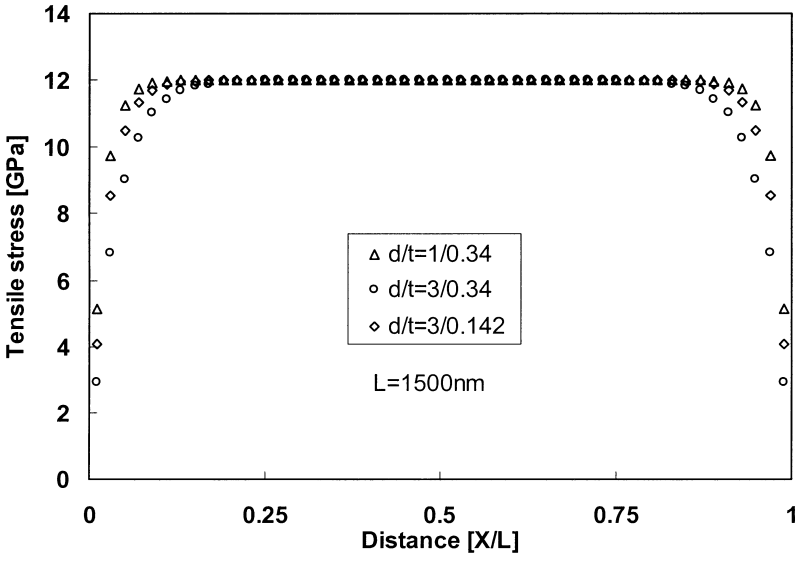

(b) L=1500nm

Figure 5 Effects of tube diameter d and wall thickness t on the tensile stress (a) $L = 100$ nm and (b) $L = 1500$ nm.

where V_c is the composite volume. The nanotube volume fraction is assumed to be constant ($R/r_2 =$ constant $= 600$). When the nanotube radius r_2 decreases, the number of nanotubes in the composite increases. Reinforcement of all nanotubes is equal to the sum of the shear force build up on the surface of each tube. Shear force induced by each tube is the integration of the shear stress over the tube surface of a half length.

Fig. 6 shows the effects of nanotube dimeter, wall thickness and length on the reinforcement of the tubes. It is seen that total shear force in the composite increases when the tube diameter decreases. Further, there seems to exist an optimal tube length at which the total shear force reaches its maximum.

2.4. Stress transfer efficiency

The ratio of σ_{tmax} to τ_{tmax}, δ, characterizes the efficiency of transferring shear stress into tensile stress through a tube-matrix interface. Fig. 7 shows the variation of δ with the tube length L, diameter d and wall thicknesses t. Clearly, δ increases with L and approaches its saturation value δ_s when L becomes infinite. It is also seen that a larger d or a smaller t (smaller t/r_2) can greatly raise δ_s.

The effect of a tube's structure and Young's modulus on the stress transfer efficiency is shown in Fig. 8. When $R/r_2 =$ constant and $r_1 = 0$ (corresponding to a solid fibre), δ_s becomes independent of the radius r_2, according to Equations 1 to 3. Assuming that a tube has carbon fibre's modulus ($E = 230$ GPa), when its structure changes from a solid one to a hollow one ($d = 3$ nm, $t = 0.142$ nm), δ_s increases from 49.5 to 117 (see curves $\times$ and -). Keeping its hollow structure unchanged but changing its modulus to its real value (1.2 TPa), δ_s increases from 117 to 267 (see curves - and ●). This shows that 69% of the difference in δ_s is caused by the value of Young's modulus and 31% is in-

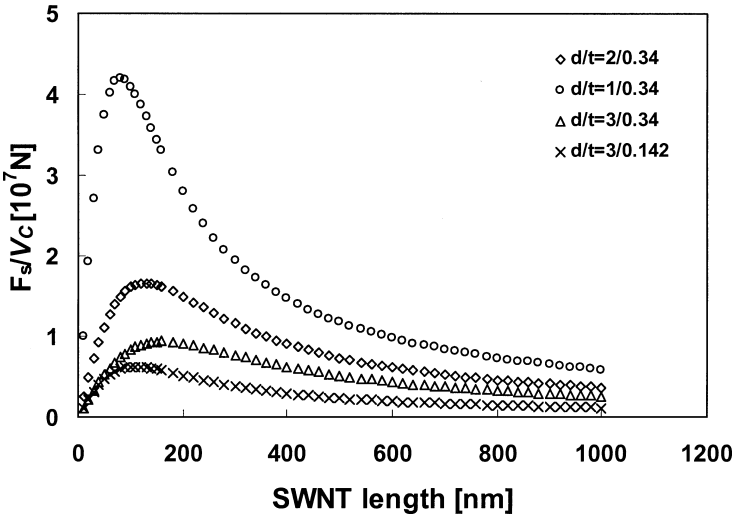

Figure 6 Total shear force F_s per unit of composite volume, V_c, as a function of tube length under various tube diameters and wall thicknesses when nanotube volume fraction is kept constant.

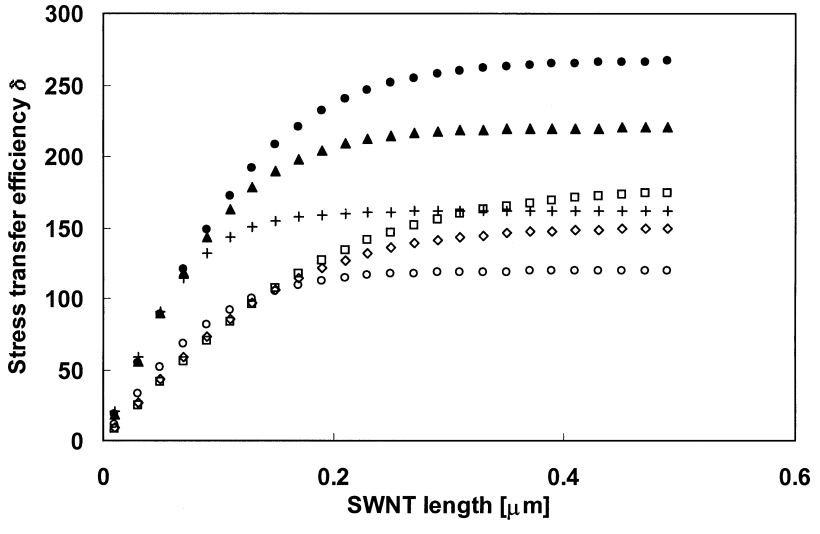

Figure 7 Effects of tube diameter and wall thickness on the stress transfer efficiency: +, $d = 1$ nm and $t = 0.142$ nm; ▲, $d = 2$ nm and $t = 0.142$ nm; ●, $d = 3$ nm and $t = 0.142$ nm; ○, $d = 1$ nm and $t = 0.34$ nm; ◇, $d = 2$ nm and $t = 0.34$ nm; □, $d = 3$ nm and $t = 0.34$ nm.

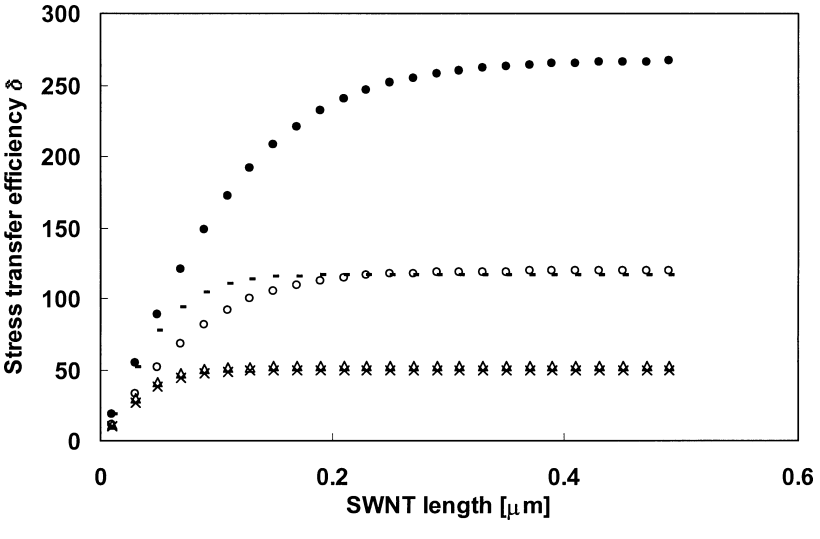

Figure 8 Effects of a tube's structure and Young's modulus on the stress transfer efficiency: ●, $d = 3$ nm and $t = 0.142$ nm; ○, $d = 1$ nm and $t = 0.34$ nm; and with Young's modulus assumed to be 230 GPa for, -, $d = 3$ nm and $t = 0.142$ nm; △, $d = 1$ nm and $t = 0.34$ nm, and ×, $d = 1$ nm and $r_1 = 0$ (δ_s = that of a carbon fibre).

duced by the structural change from solid to hollow. For another nanotube with $d = 1$ nm and $t = 0.34$ nm, calculation indicates that the contribution from tube hollow structure is only about 2% (see curves $\times$, $\triangle$ and $\circ$). It seems that the contribution of the hollow structure increases with decreasing t/r_2. Since the real wall thickness t of a nanotube can be smaller than its atomic diameter (0.142 nm) [22], the structural effect of a CNT on the δ_s of a CNT-reinforced nanocomposite can be considerable.

Because the bonding between inner and outer tubes of a multi-walled nanotube is weak [24, 25], inter-wall sliding may occur. Thus, a MWNT may be approximately treated as a SWNT in a composite system. The above discussion indicates that a MWNT should have a larger δ_s than that of a SWNT since the outer diameter of the former is usually 10 times larger.

The large stress transfer efficiency of a CNT-reinforced composite indicates that the improvement of its toughness can be achieved at a relatively low loss of its tensile strength, and vice versa, by tailoring the interfacial bonding strength. Its large δ also allows a high tensile stress to be obtained at a relatively low shear stress level, to reduce the possibility of matrix failure. These effects cannot be achieved in the usual fibre-reinforced composite [20].

3. Conclusions

The Cox model was modified and applied to assess the load transfer of CNT-reinforced composites. It was found that a smaller nanotube diameter is preferred. This study also found that there exists an optimal tube length at which the reinforcement is maximized. The stress transfer efficiency δ of a CNT-reinforced composite is much higher than that of its carbon fibre-reinforced counterpart, caused by the high Young's modulus and hollow structure of CNTs. This provides the flexibility of property optimization in terms of tensile strength and toughness of a CNT-reinforced composite.

Acknowledgement

The authors thank their colleague Dr H. Y. Liu for fruitful discussion. This work is financially supported by Australia Research Council (ARC) through a Discovery Grant.

References

1. M. M. TREACY, T. W. EBBESEN and J. M. GIBSON, *Nature* **381** (1996) 678.
2. E. W. WONG, P. E. SHEEHAN and C. M. LIEBER, *Science* **277** (1997) 1971.
3. P. ZHANG, Y. HUANG, P. H. GEUBELLE, P. A. KLEIN and K. C. HWANG, *International Journal of Solids and Structures* **39** (2002) 3893.
4. L. H. PEEBLES, in "Carbon Fibres: Formation, Structure and Properties" (CRC Press, Boca Raton, 1995).
5. H. D. WAGNER, *Chem. Phys. Lett.* **361** (2002) 57.
6. H. D. WAGNER, O. LOURIE, Y. FELDMAN and R. TENNE, *Appl. Phys. Lett.* **72** (1998) 188.
7. H. D. WAGNER and O. LOURIE, *ibid.* **73** (1998) 3527.
8. O. LOURIE and H. D. WAGNER, *Compos. Sci. Technol.* **59** (1999) 975.
9. A. KELLY and W. R. TYSON, *J. Mech. Phys. Solids* **13** (1965) 329.
10. K. LIAO and S. LI, *Appl. Phys. Lett.* **79** (2001) 4225.
11. D. QIAN, E. C. DICKEY, R. ANDREWS and T. RANTELL, *ibid.* **76** (2000) 2868.
12. D. QIAN and E. C. DICKEY, *J. Microscopy* **204** (2001) 39.
13. A. H. BARBER, S. R. COHEN and H. D. WAGNER, *Appl. Phys. Lett.* **82** (2003) 4140.
14. C. A. COOPER, S. R. COHEN, A. H. BARBER and H. D. WAGNER, *ibid.* **81** (2002) 3873.
15. P. M. AJAYAN, O. STEPHAN, C. COLLIEX and D. TRAUTH, *Science* **265** (1994) 1212.
16. L. S. SCHADLER, S. C. GIANNARIS and P. M. AJAYAN, *Appl. Phys. Lett.* **73** (1999) 3842.
17. K. T. LAU, *Chemical Phys. Lett.* **370** (2003) 399.
18. S. J. V. FRANKLAND, A. CAGLAR, D. W. BRENNER and M. GRIEBEL, *J. Phys. Chem.* **B106** (2002) 3046.
19. H. L. COX, *Brit. J. Appl. Phys.* **3** (1952) 72.
20. A. KELLY and N. H. MACMILLAN, in "Strong Solids," 3rd edn. (Clarendon Press, Oxford, 1986).
21. J. P. S. DELMOTTE and A. RUBIO, *Carbon* **40** (2002) 1729.
22. T. VODENITCHAROVA and L. C. ZHANG, *Phys. Rev.* **B68** (2003) 165401.
23. G. H. AYLWARD and T. J. V. FINDLAY, "SI Chemical Data" (John Wiley and Sons, 1974).
24. M. F. YU, O. LOURIE, M. J. DYER, K. MOLONI, T. F. KELLY and R. S. RUOFF, *Science* **287** (2000) 637.
25. M. F. YU, B. S. FILES, S. AREPALLI and R. S. RUOFF, *Phys. Rev. Lett.* **84** (2000) 5552.

Received 14 August 2003
and accepted 5 March 2004